INTERNATIONAL JOURNAL FOR NUMERICAL METHODS IN FLUIDS
Int. J. Numer. Meth. Fluids 2003; **43**:903–913 (DOI: 10.1002/fld.583)

A Reynolds-uniform numerical method for Prandtl's boundary layer problem for flow past a wedge

J. S. Butler[1], John J. H. Miller[1,*,†] and Grigorii I. Shishkin[2]

[1]*Department of Mathematics, University of Dublin, Trinity College, Dublin 2, Ireland*
[2]*Institute of Mathematics & Mechanics, Ural Branch of RAS, Ekaterinburg, Russia*

SUMMARY

In this paper, we deal with Prandtl's boundary layer problem for incompressible laminar flow past a wedge. When the Reynolds number is large the solution of this problem has a parabolic boundary layer. We construct a direct numerical method for computing approximations to the solution of this problem using a piecewise uniform fitted mesh technique appropriate to the parabolic boundary layer. We use the numerical method to approximate the self-similar solution of Prandtl's problem in a finite rectangle excluding the leading edge of the wedge, which is the source of an additional singularity caused by incompatibility of the problem data. We verify that the constructed numerical method is robust, in the sense that the computed errors for the velocity components and their derivatives in the discrete maximum norm are Reynolds uniform. We construct and apply a special numerical method related to the Falkner–Skan technique to compute a reference solution for the error analysis of the velocity components and their derivatives. By means of extensive numerical experiments we show that the constructed direct numerical method is Reynolds uniform. Copyright © 2003 John Wiley & Sons, Ltd.

KEY WORDS: boundary layer equations; Prandtl's problem for wedge; piecewise uniform mesh; Reynolds-uniform numerical method

1. INTRODUCTION

Incompressible laminar flow past a semi-infinite wedge W in the domain $D = \mathbf{R}^2/W$ is governed by the Navier–Stokes equations. Using Prandtl's approach the vertical momentum equation is omitted and the horizontal momentum equation is simplified, see References [1] and [2]. The new momentum equation is parabolic and singularly perturbed, which means that the highest order derivative is multiplied by a small singular perturbation parameter. In this case the parameter is the reciprocal of the Reynolds number. For convenience we use the notation $\varepsilon = 1/Re$.

*Correspondence to: J. J. H. Miller, Mathematics Department, Trinity College, Dublin 2, Ireland.
†E-mail: jmiller@tcd.ie

Contract/grant sponsor: Russian Foundation for Basic Research; contract/grant number: 98-01-00362
Contract/grant sponsor: Enterprise Ireland; contract/grant numbers: SC/98/612 and SC/2000/070

Received 20 April 2002
Accepted 19 February 2003

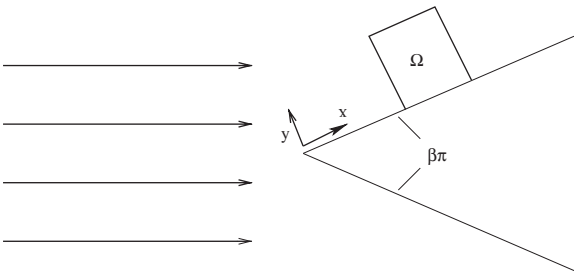

Figure 1. Flow past a wedge.

It is well-known that for flow problems with large Reynolds numbers a boundary layer arises on the surface of the wedge. Also, when classical numerical methods are applied to these problems large errors occur, especially in approximations of the derivatives, which grow unboundedly as the Reynolds number increases. For this reason robust layer-resolving numerical methods, in which the error is independent of the singular perturbation parameter, are required. We want to solve the Prandtl problem in a region including the parabolic boundary layer. Since the solution of the problem has another singularity at the leading edge of the wedge we take as the computational domain the finite rectangle $\Omega = (.1, 1.1) \times (0, 1)$ on the upper side of the wedge (see Figure 1). This is sufficiently far from the leading edge that the leading edge singularity does not cause problems for the numerical method. We denote the boundary of Ω by $\Gamma = \Gamma_L \cup \Gamma_T \cup \Gamma_B \cup \Gamma_R$ where Γ_L, Γ_T, Γ_B and Γ_R denote, respectively the left-hand, top, bottom and right-hand edges of Ω.

The Prandtl boundary layer problem in D is:

$$(P_\varepsilon)\begin{cases} \text{Find } \mathbf{u}_\varepsilon = (u_\varepsilon, v_\varepsilon) \text{ such that for all } (x, y) \in D \\ \mathbf{u}_\varepsilon \text{ satisfies the differential equation} \\ -\dfrac{1}{Re}\dfrac{\partial^2 u_\varepsilon}{\partial^2 y} + \mathbf{u}_\varepsilon.\nabla u_\varepsilon = U\dfrac{\mathrm{d}U}{\mathrm{d}x} \\ \nabla.\mathbf{u}_\varepsilon = 0 \\ \text{with boundary conditions} \\ \mathbf{u}_\varepsilon = 0 \text{ on } \Gamma_B \\ \mathbf{u}_\varepsilon = \mathbf{u}_P \text{ on } \Gamma_L \cup \Gamma_T \end{cases}$$

where $U(x) = x^m$ is the solution of the reduced problem ($\varepsilon = 0$), $m = \beta/(2-\beta)$ and $\beta\pi$ is the angle in radians of the wedge.

Our goal here is to construct an (Re, β)-uniform numerical method for solving P_ε. That is a method having error bounds for the solution and its derivatives independent of Re and β, for all $Re \in [1, \infty)$ and all $\beta \in [0, 1]$.

2. FALKNER–SKAN SIMILARITY SOLUTION

Using the similarity transformation described (for example, in Reference [3])

$$\eta = y\sqrt{\frac{(m+1)Re}{2}\frac{U}{x}}$$

the velocity components of the Falkner–Skan solution $\mathbf{u}_{\mathrm{FS}}$ of (P_ε) are given by

$$u_{\mathrm{FS}}(x,y) = u_1 x^m f'(\eta) = U f'(\eta)$$

$$v_{\mathrm{FS}}(x,y) = -\sqrt{\frac{m+1}{2x}\frac{U}{Re}}\left(f + \frac{m-1}{m+1}\eta f'\right)$$

where f is the solution of the non-linear ordinary differential equation

$$(P_{\mathrm{FS}})\begin{cases} \text{For } \eta \in (0,\infty) \text{ find } f \in C^3(0,\infty) \\ f''' + ff'' + \beta(1-f'^2) = 0 \\ \text{with boundary conditions} \\ f(0) = f'(0) = 0, \quad f'(\infty) = 1 \end{cases}$$

To find the components $u_{\mathrm{FS}}(x,y)$, $v_{\mathrm{FS}}(x,y)$ of $\mathbf{u}_{\mathrm{FS}}$, and their derivatives, on the finite domain Ω for all $Re \in [1,\infty)$, we need to solve (P_{FS}) numerically for $f(\eta)$ and its derivatives on the semi-infinite domain $[0,\infty)$. Then we apply postprocessing to determine numerical approximations to $\mathbf{u}_{\mathrm{FS}}$. This process is described in detail in Reference [4] for flow past a flat plate.

Here, we make use of the Falkner–Skan similarity solution of Prandtl's problem in two ways. First, we use it to provide the unknown boundary conditions that are required on the boundary of Ω in the direct numerical method for Prandtl's problem discussed in the next section. Secondly, we use it as a reference solution for the unknown exact solution in the expression for the error. Since the Falkner–Skan solution is known to converge Reynolds uniformly to the solution of Prandtl's problem, we can compute Reynolds uniform error bounds. For this purpose we find that the Falkner–Skan solution for (P_{FS}) with $N = 8192$, namely $\mathbf{U}_{\mathrm{FS}}^{8192}$, provides the required accuracy for the velocity components U_{FS}^{8192}, V_{FS}^{8192} and their scaled discrete derivatives $\sqrt{\varepsilon}D_y U_{\mathrm{FS}}^{8192}$, $D_x V_{\mathrm{FS}}^{8192}$ and $D_y V_{\mathrm{FS}}^{8192}$.

3. DIRECT NUMERICAL METHOD FOR PRANDTL'S PROBLEM

The aim of this section is to construct a direct numerical method to solve the Prandtl problem (P_ε) for all $Re \in [1,\infty)$ and all $\beta \in [0,1]$. We require a piecewise uniform fitted mesh $\Omega_\varepsilon^{\mathrm{N}}$ in the rectangle Ω. It is important to note the location and width of the boundary layer in order to determine where to place and to choose an appropriate transition point from the coarse to the fine mesh. We define the mesh as the tensor product of two one-dimensional meshes. The mesh in the x direction is the uniform mesh.

$$\Omega_u^{N_x} = \{x_i : x_i = 0.1 + iN_x^{-1},\ 0 \leqslant i \leqslant N_x\}$$

The mesh in the y-direction is the piecewise uniform fitted mesh

$$\Omega_\varepsilon^{N_y} = \left\{ y_j : y_j = \sigma j \frac{2}{N_y},\ 0 \leqslant j \leqslant \frac{N_y}{2};\ \ y_j = \sigma + (1-\sigma)\left(j - \frac{N_y}{2}\right)\frac{2}{N_y}, \frac{N_y}{2} \leqslant j \leqslant N_y \right\}$$

where the transition point σ is chosen so that there is a fine mesh in the boundary layer whenever it is required. The appropriate choice in this case is

$$\sigma = \min\left\{ \frac{1}{2}, \sqrt{\varepsilon}\ \ln N_y \right\}$$

The factor $\sqrt{\varepsilon}$ may be motivated from *a priori* estimates of the derivatives of the solution $\mathbf{u}_\varepsilon$ or from asymptotic analysis. The rectangular mesh on Ω is then the tensor product $\Omega_\varepsilon^N = 1\Omega_u^{N_u} \times \Omega_\varepsilon^{N_y}$, where $\mathbf{N} = (N_x, N_y)$. For simplicity we take $N_x = N_y = N$.

The problem (P_ε) is discretized by the following non-linear upwind finite difference method on the piecewise uniform fitted mesh Ω_ε^N

$$(P_\varepsilon^N)\begin{cases} \text{Find } \mathbf{U}_\varepsilon = (U_\varepsilon, V_\varepsilon) \text{ such that for all } (x_i, y_j) \in \Omega_\varepsilon^N \\ \mathbf{U}_\varepsilon \text{ satisfies the finite difference equations} \\ -\varepsilon\delta_y^2 U_\varepsilon(x_i, y_j) + U_\varepsilon(x_i, y_j) D_x^- U_\varepsilon(x_i, y_j) \\ +V_\varepsilon(x_i, y_j) D_y^u U_\varepsilon(x_i, y_j) = U(x_i)\dfrac{\mathrm{d}U}{\mathrm{d}x}(x_i) \\ D_x^- U_\varepsilon(x_i, y_j) + D_y^- V_\varepsilon(x_i, y_j) = 0 \\ \text{with boundary conditions} \\ \mathbf{U}_\varepsilon = 0 \text{ on } \Gamma_B \\ \mathbf{U}_\varepsilon = \mathbf{U}_{\mathrm{FS}} \text{ on } \Gamma_L \cup \Gamma_T \end{cases}$$

where D_x^-, D_x^+ and D_y^-, D_y^+ are the standard first-order backward, respectively forward, finite difference operators in the x and y directions and, for any continuous function $V_\varepsilon(x_i, y_j)$ on the domain Ω_ε^N, D_y^u is defined by

$$V_\varepsilon(x_i, y_j) D_y^u U_\varepsilon(x_i, y_j) = \begin{cases} V_\varepsilon(x_i, y_j) D_y^- U_\varepsilon(x_i, y_j) & \text{if } V_\varepsilon(x_i, y_j) \geqslant 0 \\ V_\varepsilon(x_i, y_j) D_y^+ U_\varepsilon(x_i, y_j) & \text{if } V_\varepsilon(x_i, y_j) < 0 \end{cases}$$

δ_y^2 is the standard second-order centred difference operator in the y direction. Changes between forward and backward differences are required because at angles $\beta > 0.1$, V_ε is initially negative and then becomes positive. This means that, without these changes, the tridiagonal system is no longer diagonally dominant and the continuation algorithm fails to converge.

Since (P_ε^N) is a non-linear finite difference method an iterative method is required for its solution. This is obtained by replacing the system of non-linear equations by the following

sequence of systems of linearized equations:

$$(A_\varepsilon^N)\begin{cases}\text{With the boundary condition } \mathbf{U}_\varepsilon^{\mathrm{M}} = \mathbf{U}_{\mathrm{FS}}^{8192} \text{ on } \Gamma_{\mathrm{L}},\\ \text{for each } i,\ 1 \leqslant i \leqslant N, \text{ use the initial guess } \mathbf{U}_\varepsilon^0|_{X_i} = \mathbf{U}_\varepsilon^{M_{i-1}}|_{X_{i-1}}\\ \text{and for } m = 1, \ldots, M_i \text{ solve the following}\\ \text{two-point boundary value problem for } U_\varepsilon^m(x_i, y_j)\\ (-\varepsilon\delta_y^2 + \mathbf{U}_\varepsilon^{m-1} \cdot \mathbf{D}^-)U_\varepsilon^m(x_i, y_j) = (U\tfrac{\mathrm{d}U}{\mathrm{d}x})(x_i), \quad 1 \leqslant j \leqslant N-1\\ \text{with the boundary conditions } U_\varepsilon^m = U_{\mathrm{FS}}^{8192} \text{ on } \Gamma_{\mathrm{B}} \cup \Gamma_{\mathrm{T}},\\ \text{and the initial guess for } V_\varepsilon^0|_{X_1} = 0\\ \text{Also solve the initial value problem for } V_\varepsilon^m(x_i, y_j)\\ (\mathbf{D}^- \cdot \mathbf{U}_\varepsilon^m)(x_i, y_j) = 0,\\ \text{with initial condition } V_\varepsilon^m = 0 \text{ on } \Gamma_{\mathrm{B}}.\\ \text{Continue to iterate between the equations for } \mathbf{U}_\varepsilon^m \text{ until } m = M_i,\\ \text{where } M_i \text{ is such that}\\ \max(|U_\varepsilon^{M_i} - U_\varepsilon^{M_i-1}|_{\bar{X}_i}, \tfrac{1}{V^*}|V_\varepsilon^{M_i} - V_\varepsilon^{M_i-1}|_{\bar{X}_i}) \leqslant \mathrm{tol}\end{cases}$$

For notational simplicity, we suppress explicit mention of the iteration superscript M_i henceforth, and we write simply $\mathbf{U}_\varepsilon$ for the solution generated by (A_ε^N). We take $\mathrm{tol} = 10^{-6}$ in the computations. We note that there are no known theoretical results concerning the convergence of the solutions $\mathbf{U}_\varepsilon$ of (P_ε^N) to the solution $\mathbf{u}_\varepsilon$ of (P_ε) and no theoretical estimate for the pointwise error $(\mathbf{U}_\varepsilon - \mathbf{u}_\varepsilon)(x_i, y_j)$. It is for this reason that we are forced to apply controllable experimental techniques, which are adapted to the problem under consideration. These are of crucial value to our understanding of the computationally problems and are the topic of the next section.

4. ERROR ANALYSIS

In this section, we compute Reynolds-uniform maximum pointwise errors in the approximations generated by the direct numerical method described in the previous section. For the sake of brevity, we show the errors for just one typical value of the angle of the wedge, $\beta = 0.6$. The appropriate scaling factor for the vertical velocity is

$$V^* = \max_{\Omega_\varepsilon^N} V_{\mathrm{FS}}^{8192}$$

We compare the approximations generated by the direct numerical methods A_ε^N of the previous section with the corresponding values of U_{FS}^{8192}. We use the following difinitions for the computed errors

$$E_\varepsilon^N(U_\varepsilon) = ||U_\varepsilon - \overline{U_{\mathrm{FS}}^{8192}}||_{\bar{\Omega}_\varepsilon^N}$$

$$E_\varepsilon^N\left(\frac{1}{V^*}\, V_\varepsilon\right) = \frac{1}{V^*}\, ||V_\varepsilon - \overline{V_{\mathrm{FS}}^{8192}}||_{\bar{\Omega}_\varepsilon^N}$$

Table I. Computed maximum pointwise error $E_\varepsilon^N(U_\varepsilon)$ where U_ε is generated by (A_ε^N) for various values of ε, N and $\beta = 0.6$.

$\varepsilon \backslash N$	8	16	32	64	128	256	512
2^{-0}	1.804e-03	1.344e-03	7.610e-04	4.369e-04	2.418e-04	1.324e-04	7.488e-05
2^{-2}	1.389e-02	8.192e-03	4.506e-03	2.402e-03	1.239e-03	6.274e-04	3.137e-04
2^{-4}	3.000e-02	1.663e-02	8.862e-03	4.577e-03	2.321e-03	1.161e-03	5.726e-04
2^{-6}	3.244e-02	1.972e-02	1.095e-02	5.680e-03	2.855e-03	1.422e-03	7.002e-04
2^{-8}	3.292e-02	1.933e-02	1.106e-02	5.803e-03	2.966e-03	1.502e-03	7.519e-04
2^{-10}	3.521e-02	1.924e-02	1.100e-02	5.799e-03	2.966e-03	1.502e-03	7.519e-04
2^{-12}	4.560e-02	1.927e-02	1.096e-02	5.796e-03	2.966e-03	1.502e-03	7.519e-04
2^{-14}	5.100e-02	1.930e-02	1.094e-02	5.794e-03	2.966e-03	1.502e-03	7.519e-04
2^{-16}	5.375e-02	1.932e-02	1.093e-02	5.793e-03	2.966e-03	1.502e-03	7.519e-04
2^{-18}	5.513e-02	1.933e-02	1.092e-02	5.792e-03	2.966e-03	1.502e-03	7.519e-04
2^{-20}	5.583e-02	1.933e-02	1.092e-02	5.792e-03	2.966e-03	1.502e-03	7.519e-04

Table II. Computed maximum pointwise error $E_\varepsilon^N(\frac{1}{V^*}V_\varepsilon)$ where V_ε is generated by (A_ε^N) for various values of ε, N and $\beta = 0.6$.

$\varepsilon \backslash N$	8	16	32	64	128	256	512
2^{-0}	3.064e-02	2.034e-02	1.150e-02	6.118e-03	3.308e-03	1.831e-03	1.066e-03
2^{-2}	2.530e-02	1.435e-02	7.258e-03	3.736e-03	1.941e-03	1.027e-03	5.658e-04
2^{-4}	1.995e-02	1.112e-02	5.508e-03	2.793e-03	1.429e-03	7.412e-04	3.955e-04
2^{-6}	1.648e-02	9.162e-03	4.739e-03	2.519e-03	1.280e-03	6.538e-04	3.389e-04
2^{-8}	1.474e-02	7.736e-03	3.779e-03	1.964e-03	1.033e-03	5.451e-04	2.895e-04
2^{-10}	1.385e-02	7.068e-03	3.332e-03	1.687e-03	8.702e-04	4.493e-04	2.329e-04
2^{-12}	1.339e-02	6.744e-03	3.116e-03	1.559e-03	7.919e-04	4.034e-04	2.059e-04
2^{-14}	1.316e-02	6.584e-03	3.010e-03	1.495e-03	7.539e-04	3.809e-04	1.926e-04
2^{-16}	1.304e-02	6.505e-03	2.957e-03	1.464e-03	7.350e-04	3.698e-04	1.861e-04
2^{-18}	1.298e-02	6.465e-03	2.931e-03	1.448e-03	7.256e-04	3.642e-04	1.828e-04
2^{-20}	1.295e-02	6.445e-03	3.918e-03	1.440e-03	7.209e-04	3.615e-04	1.812e-04

The numerical results in Tables I and II, respectively, indicate that the method is Reynolds uniform for the scaled velocity components U_ε and $(1/V^*)V_\varepsilon$.

In Figure 2 we see that the computed scaled velocity components have no non-physical oscillations. The boundary layer on the surface of the wedge is apparent for the horizontal velocity component U_ε.

We define the computed local order of convergence $p_{\varepsilon,\mathrm{comp}}^N$ for the horizontal velocity component U_ε^N by

$$p_{\varepsilon,\mathrm{comp}}^N = \log_2 \frac{||U_\varepsilon^N - \overline{U_{\mathrm{FS}}^{8192}}||_{\Omega_\varepsilon^N}}{||U_\varepsilon^{2N} - \overline{U_{\mathrm{FS}}^{8192}}||_{\Omega_\varepsilon^{2N}}}$$

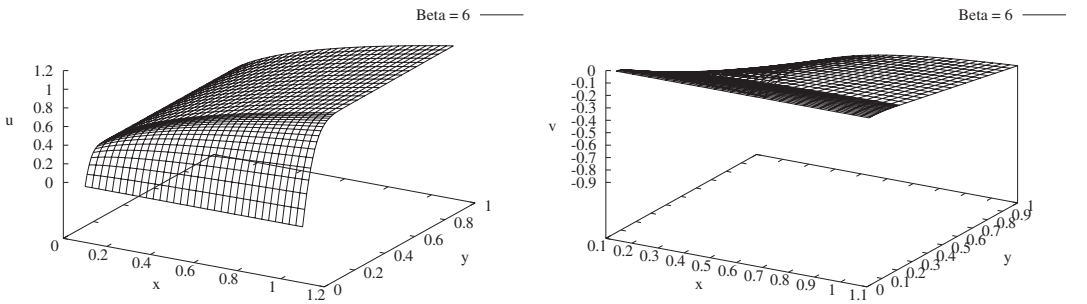

Figure 2. Graphs of U_ε^N and $\frac{1}{V^*}V_\varepsilon^N$ for $\varepsilon = 2^{-8}$, $N = 32$ and $\beta = 0.6$.

Table III. Computed orders of convergence $p^N_{\varepsilon,\mathrm{comp}}$, p^N_{comp} for $U_\varepsilon - \overline{U^{8192}_{\mathrm{FS}}}$ where U_ε is generated by (A^N_ε) for various values of ε, N and $\beta = 0.6$.

$\varepsilon \backslash N$	8	16	32	64	128	256
2^{-0}	0.42	0.82	0.80	0.85	0.87	0.82
2^{-2}	0.76	0.86	0.91	0.95	0.98	1.00
2^{-4}	0.85	0.91	0.95	0.98	1.00	1.02
2^{-6}	0.72	0.85	0.95	0.99	1.01	1.02
2^{-8}	0.77	0.81	0.93	0.97	0.98	1.00
2^{-10}	0.87	0.81	0.92	0.97	0.98	1.00
2^{-12}	1.24	0.81	0.92	0.97	0.98	1.00
2^{-14}	1.40	0.82	0.92	0.97	0.98	1.00
2^{-16}	1.48	0.82	0.92	0.97	0.98	1.00
2^{-18}	1.51	0.82	0.92	0.97	0.98	1.00
2^{-20}	1.53	0.82	0.92	0.97	0.98	1.00
p^N_{comp}	1.50	0.83	0.93	0.97	0.98	1.00

and the ε-uniform order p^N_{comp} by

$$p^N_{\mathrm{comp}} = \log_2 \frac{\max_\varepsilon ||U^N_\varepsilon - \overline{U^{8192}_{\mathrm{FS}}}||_{\Omega^N_\varepsilon}}{\max_\varepsilon ||U^{2N}_\varepsilon - \overline{U^{8192}_{\mathrm{FS}}}||_{\Omega^{2N}_\varepsilon}}$$

with analogous expressions for the vertical velocity V^N_ε. The Tables III and IV we give the numerical results for these computed ε-uniform orders of convergence.

We see that for all $N \geqslant 16$ the order of convergence for the approximations to the scaled velocity components in each case is at least 0.78. This indicates that for the velocity components the method is Reynolds uniform for $\beta = 0.6$.

The graphs in Figure 3 show where the error in the scaled velocity components is largest. For the horizontal component this is at points in the boundary layer on the surface of the wedge and for the vertical component it is at points farthest from the surface of the wedge on the side of the computational domain closest to the leading edge.

Table IV. Computed orders of convergence $p^N_{\varepsilon,\mathrm{comp}}$, p^N_{comp} for $\frac{1}{V^*}(V_\varepsilon - \overline{V^{8192}_{\mathrm{FS}}})$ where V_ε is generated by (A^N_ε) for various values of ε, N and $\beta = 0.6$.

$\varepsilon \backslash N$	8	16	32	64	128	256
2^{-0}	0.59	0.82	0.91	0.89	0.85	0.78
2^{-2}	0.82	0.98	0.96	0.94	0.92	0.86
2^{-4}	0.84	1.01	0.98	0.97	0.95	0.91
2^{-6}	0.85	0.95	0.91	0.98	0.97	0.95
2^{-8}	0.93	1.03	0.94	0.93	0.92	0.91
2^{-10}	0.97	1.08	0.98	0.96	0.95	0.95
2^{-12}	0.99	1.11	1.00	0.98	0.97	0.97
2^{-14}	1.00	1.13	1.01	0.99	0.99	0.98
2^{-16}	1.00	1.14	1.01	0.99	0.99	0.99
2^{-18}	1.01	1.14	1.02	1.00	0.99	0.99
2^{-20}	1.01	1.14	1.02	1.00	1.00	1.00
p^N_{comp}	0.59	0.82	0.91	0.89	0.85	0.78

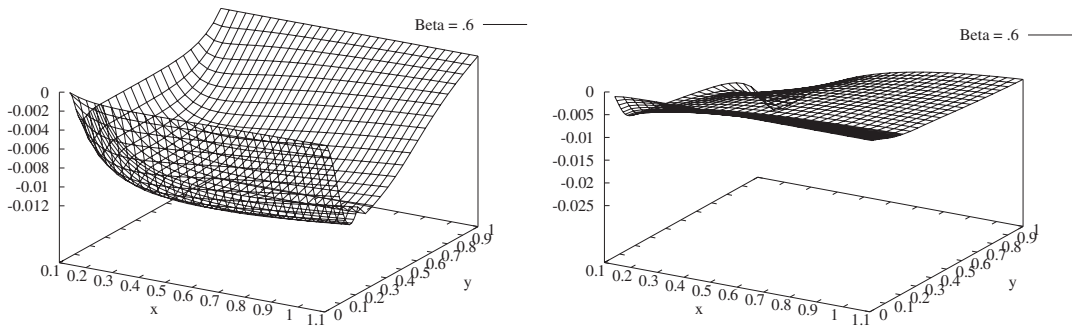

Figure 3. Graphs of $U_\varepsilon - U_{\mathrm{FS}}$ and $(1/V^*)(V_\varepsilon - V_{\mathrm{FS}})$ for $\varepsilon = 2^{-8}$, $N = 32$ and $\beta = 0.6$.

In Tables V–VII we display the computed maximum pointwise errors in the approximations to the scaled first-order derivatives of the velocity components. Since $D_y V = -D_x U$ it is only necessary to show the errors for one of these. Further computations, not reported here, show that the errors for the scaled derivatives reduce as the angle β tends to 1, because the singularity at the leading edge has less effect. All of these numerical experiments indicate that the method is (Re, β)-uniform for all $Re \in [1, \infty)$ and all $\beta \in [0, 1]$.

In Tables VIII–X we display the computed orders of convergence for the approximations of the first-order derivatives to the scaled velocity components $D^-_x V_\varepsilon, D^-_y V_\varepsilon$ and $\sqrt{\varepsilon} D^-_y U_\varepsilon$ obtained, respectively, from the corresponding Tables V–VII. We see that for each value of N the orders of convergence stabilize as $\varepsilon \to 0$ for $\beta = 0.6$. In additional computations, not reported here, similar behaviour is observed for all $\beta \in [0, 1]$.

Table V. Computed maximum pointwise scaled error $\sqrt{\varepsilon}||D_y^- U_\varepsilon - D_y \overline{U_{\mathrm{FS}}^{8192}}||_{\overline{\Omega_\varepsilon^N}/\Gamma_L}$ where U_ε is generated by (A_ε^N) for various values of ε, N and $\beta = 0.6$.

$\varepsilon\backslash N$	8	16	32	64	128	256	512
2^{-2}	7.367e-02	3.745e-02	1.896e-02	9.669e-03	5.052e-03	2.784e-03	1.736e-03
2^{-4}	1.394e-01	7.367e-02	3.745e-02	1.896e-02	9.669e-03	5.052e-03	2.784e-03
2^{-6}	1.440e-01	1.004e-01	6.414e-02	3.745e-02	1.911e-02	9.759e-03	5.052e-03
2^{-8}	1.440e-01	1.004e-01	6.414e-02	3.891e-02	2.316e-02	1.343e-02	7.713e-03
2^{-10}	1.440e-01	1.004e-01	6.414e-02	3.891e-02	2.316e-02	1.343e-02	7.713e-03
2^{-12}	1.440e-01	1.004e-01	6.414e-02	3.891e-02	2.316e-02	1.343e-02	7.713e-03
2^{-14}	1.440e-01	1.004e-01	6.414e-02	3.891e-02	2.316e-02	1.343e-02	7.713e-03
2^{-16}	1.440e-01	1.004e-01	6.414e-02	3.891e-02	2.316e-02	1.343e-02	7.713e-03
2^{-18}	1.440e-01	1.004e-01	6.414e-02	3.891e-02	2.316e-02	1.343e-02	7.713e-03
2^{-20}	1.440e-01	1.004e-01	6.414e-02	3.891e-02	2.316e-02	1.343e-02	7.713e-03

Table VI. Computed maximum pointwise error $||D_y^- V_\varepsilon - D_y \overline{V_{\mathrm{FS}}^{8192}}||_{\overline{\Omega_\varepsilon^N}}$ where V_ε is generated by (A_ε^N) for various values of ε, N and $\beta = 0.6$.

$\varepsilon\backslash N$	8	16	32	64	128	256	512
2^{-2}	2.548e-01	1.811e-01	1.131e-01	6.435e-02	3.451e-02	1.788e-02	9.082e-03
2^{-4}	2.802e-01	1.690e-01	1.068e-01	6.118e-02	3.295e-02	1.713e-02	8.736e-03
2^{-6}	2.929e-01	2.093e-01	1.320e-01	7.711e-02	3.946e-02	2.072e-02	1.135e-02
2^{-8}	2.929e-01	2.093e-01	1.320e-01	8.007e-02	4.748e-02	2.789e-02	1.654e-02
2^{-10}	2.929e-01	2.093e-01	1.320e-01	8.007e-02	4.748e-02	2.789e-02	1.654e-02
2^{-12}	2.929e-01	2.093e-01	1.320e-01	8.007e-02	4.748e-02	2.789e-02	1.654e-02
2^{-14}	2.929e-01	2.093e-01	1.320e-01	8.007e-02	4.748e-02	2.789e-02	1.654e-02
2^{-16}	2.929e-01	2.093e-01	1.320e-01	8.007e-02	4.748e-02	2.789e-02	1.654e-02
2^{-18}	2.929e-01	2.093e-01	1.320e-01	8.007e-02	4.748e-02	2.789e-02	1.654e-02
2^{-20}	2.929e-01	2.093e-01	1.320e-01	8.007e-02	4.748e-02	2.789e-02	1.654e-02

Table VII. Computed maximum pointwise scaled error $V^{*-1}||D_x^- V_\varepsilon - D_x \overline{V_{\mathrm{FS}}^{8192}}||_{\overline{\Omega_\varepsilon^N}}$ where V_ε is generated by (A_ε^N) for various values of ε, N and $\beta = 0.6$.

$\varepsilon\backslash N$	8	16	32	64	128	256	512
2^{-2}	8.756e-01	8.233e-01	6.212e-01	3.909e-01	2.419e-01	1.636e-01	7.728e-02
2^{-4}	6.436e-01	6.646e-01	5.492e-01	3.795e-01	2.521e-01	1.761e-01	1.116e-01
2^{-6}	5.860e-01	6.019e-01	5.048e-01	3.652e-01	2.575e-01	1.828e-01	1.255e-01
2^{-8}	5.661e-01	5.714e-01	4.642e-01	3.184e-01	2.210e-01	1.592e-01	1.145e-01
2^{-10}	5.595e-01	5.585e-01	4.457e-01	2.950e-01	1.925e-01	1.291e-01	8.457e-02
2^{-12}	5.570e-01	5.525e-01	4.369e-01	2.838e-01	1.785e-01	1.144e-01	7.007e-02
2^{-14}	5.560e-01	5.496e-01	4.326e-01	2.782e-01	1.716e-01	1.071e-01	6.292e-02
2^{-16}	5.556e-01	5.482e-01	4.305e-01	2.755e-01	1.682e-01	1.035e-01	5.937e-02
2^{-18}	5.553e-01	5.475e-01	4.294e-01	2.741e-01	1.665e-01	1.017e-01	5.760e-02
2^{-20}	5.552e-01	5.472e-01	4.289e-01	2.734e-01	1.656e-01	1.008e-01	5.672e-02

Table VIII. Computed orders of convergence $p^N_{\varepsilon,\mathrm{comp}}$, p^N_{comp} for $\sqrt{\varepsilon}(D_y^- U_\varepsilon - D_y \overline{U^{8192}_{\mathrm{FS}}})$ where U_ε is generated by (A^N_ε) for various values of ε, N and $\beta = 0.6$.

$\varepsilon \backslash N$	8	16	32	64	128	256
2^{-2}	0.98	0.98	0.97	0.94	0.86	0.68
2^{-4}	0.92	0.98	0.98	0.97	0.94	0.86
2^{-6}	0.52	0.65	0.78	0.97	0.97	0.95
2^{-8}	0.52	0.65	0.72	0.75	0.79	0.80
2^{-10}	0.52	0.65	0.72	0.75	0.79	0.80
2^{-12}	0.52	0.65	0.72	0.75	0.79	0.80
2^{-14}	0.52	0.65	0.72	0.75	0.79	0.80
2^{-16}	0.52	0.65	0.72	0.75	0.79	0.80
2^{-18}	0.52	0.65	0.72	0.75	0.79	0.80
2^{-20}	0.52	0.65	0.72	0.75	0.79	0.80
p^N_{comp}	0.52	0.65	0.72	0.75	0.79	0.80

Table IX. Computed orders of convergence $p^N_{\varepsilon,\mathrm{comp}}$, p^N_{comp} for $D_y^- V_\varepsilon - D_y \overline{V^{8192}_{\mathrm{FS}}}$ where V_ε is generated by (A^N_ε) for various values of ε, N and $\beta = 0.6$.

$\varepsilon \backslash N$	8	16	32	64	128	256
2^{-2}	0.49	0.68	0.81	0.90	0.95	0.98
2^{-4}	0.73	0.66	0.80	0.89	0.94	0.97
2^{-6}	0.48	0.66	0.78	0.97	0.93	0.87
2^{-8}	0.48	0.66	0.72	0.75	0.77	0.75
2^{-10}	0.48	0.66	0.72	0.75	0.77	0.75
2^{-12}	0.48	0.66	0.72	0.75	0.77	0.75
2^{-14}	0.48	0.66	0.72	0.75	0.77	0.75
2^{-16}	0.48	0.66	0.72	0.75	0.77	0.75
2^{-18}	0.48	0.66	0.72	0.75	0.77	0.75
2^{-20}	0.48	0.66	0.72	0.75	0.77	0.75
p^N_{comp}	0.48	0.66	0.72	0.75	0.77	0.75

5. CONCLUSION

We considered Prandtl's boundary layer equations for incompressible laminar flow past a wedge with angle $\beta\pi$, $\beta \in [0, 1]$. When the Reynolds number is large the solution of this problem has a parabolic boundary layer on the surface of the wedge. We constructed a direct numerical method for computing approximations to the solution of this problem using a piecewise uniform fitted mesh technique appropriate for this parabolic boundary layer. We used the method to approximate the self-similar solution of Prandtl's problem, in a finite rectangular computational domain excluding the leading edge of the wedge, for various values of Re and β. We constructed and applied a special numerical method, related to the

Table X. Computed orders of convergence $p^N_{\varepsilon,\mathrm{comp}}$, p^N_{comp} for $\frac{1}{V^*}(D_x^- V_\varepsilon - D_x \overline{V^{8192}_{\mathrm{FS}}})$ where V_ε is generated by (A^N_ε) for various values of ε, N and $\beta = 0.6$.

$\varepsilon \backslash N$	8	16	32	64	128	256
2^{-2}	0.09	0.41	0.67	0.69	0.56	1.08
2^{-4}	−0.05	0.28	0.53	0.59	0.52	0.66
2^{-6}	−0.04	0.25	0.47	0.50	0.49	0.54
2^{-8}	−0.01	0.30	0.54	0.53	0.47	0.48
2^{-10}	0.00	0.33	0.60	0.62	0.58	0.61
2^{-12}	0.01	0.34	0.62	0.67	0.64	0.71
2^{-14}	0.02	0.35	0.64	0.70	0.68	0.77
2^{-16}	0.02	0.35	0.64	0.71	0.70	0.80
2^{-18}	0.02	0.35	0.65	0.72	0.71	0.82
2^{-20}	0.02	0.35	0.65	0.72	0.72	0.83
p^N_{comp}	0.09	0.41	0.67	0.60	0.49	0.54

Falkner–Skan technique, to compute reference solutions to the Prandtl. These were used to obtain approximate boundary conditions on the non-physical boundaries of the computational domain and in the error analysis of the velocity components and their derivatives. Extensive numerical experiments indicated that the constructed direct numerical method is *Re* and β uniform.

ACKNOWLEDGEMENTS

This research was supported in part by the Enterprise Ireland grants SC-98-612 and SC/2000/070/ and by the Russian Foundation for Basic Research under grant No. 01-01-01022.

REFERENCES

1. Schlichting H. *Boundary Layer Theory* (7th edn). McGraw Hill: New York, 1951.
2. Acheson DJ. *Elementary Fluid Dynamics*. Clarendon: Oxford, 1990.
3. Rogers DF. *Laminar Flow Analysis*. Cambridge University Press: Cambridge, 1992.
4. Farrell P, Hegarty A, Miller JJH, O'Riordan E, Shishkin GI. *Robust Computational Techniques for Boundary Layers*. Chapman and Hall/CRC Press: London/Boca Raton, 2000.

